Chinese Chemical Letters 32 (2021) 3377–3381

Contents lists available at ScienceDirect

Chinese Chemical Letters

journal homepage: www.elsevier.com/locate/cclet

Communication

Significantly influenced photocatalytic performance for H_2O_2 generation over ultrathin g-C_3N_4 through regulating the migration orientation of photogenerated charge carriers

Xinxia He[a,1], Hongyan Shang[a,b,1], Chuan Wang[a], Le Chen[a], Zehan Gong[a], Jun Wang[c], Shilin Zhao[b,*], Jun Ma[a,b,*]

[a] College of Chemistry and Materials Science, Sichuan Normal University, Chengdu 610068, China
[b] Key Laboratory of Land Resources Evaluation and Monitoring in Southwest, Ministry of Education of China, Chengdu 610066, China
[c] State Key Laboratory of Environmental-Friendly Energy Materials, School of Materials Science and Engineering, Southwest University of Science and Technology, Mianyang 621010, China

ARTICLE INFO

Article history:
Received 11 January 2021
Revised 8 February 2021
Accepted 16 April 2021
Available online 22 April 2021

Keywords:
Ultra-thin g-C_3N_4
Photocatalytic H_2O_2 production
Photogenerated charge carriers
Migration orientation

ABSTRACT

H_2O_2 has been widely applied in the fields of chemical synthesis, medical sterilization, pollutant removal, etc., due to its strong oxidizing property and the avoidable secondary pollution. Despite of the enhanced performance for H_2O_2 generation over g-C_3N_4 semiconductors through promoting the separation of photo-generated charge carriers, the effect of migration orientation of charge carriers is still ambiguous. For this emotion, surface modification of g-C_3N_4 was employed to adjust the migration orientation of charge carriers, in order to investigate systematically its effect on the performance of H_2O_2 generation. It was found that ultrathin g-C_3N_4 (UCN) modified by boron nitride (BN), as an effective hole-attract agent, demonstrated a significantly enhanced performance. Particularly, for the optimum UCN/BN-40% catalyst, 4.0-fold higher yield of H_2O_2 was obtained in comparison with the pristine UCN. As comparison, UCN modified by carbon dust demonstrated a completely opposite tendency. The remarkably improved performance over UCN/BN was ascribed to the fact that more photo-generated electrons were remained inside of triazine structure of g-C_3N_4, leading to the formation of larger amount of 1,4-endoxide. It is anticipated that our work could provide new insights for the design of photocatalyst with significantly improved performance for H_2O_2 generation.

Hydrogen peroxide (H_2O_2), as a high-value and growing demanded chemical, has received extensive attention in the fields of liquid fuel cells, organic synthesis, environmental remediation, clinical medicine and water disinfection, *etc.* [1–7]. Currently, solar-driven H_2O_2 production has attracted much attention from the scientific community since solar is exhaustive resource on the earth. Particularly, the environment and safety risks for the production and transportation of H_2O_2 could be successfully avoided since these procedures are green and environmentally benign [8]. Therefore, it is of great significance to explore photocatalysts with high performance for H_2O_2 generation.

At present, various semiconductors have been applied in photocatalytic H_2O_2 generation, including TiO_2, $BiVO_4$, $CuWO_4$ and ZnO, *etc.* [9–12]. Among them, g-C_3N_4, as a metal-free polymer semiconductor, has been gradually becoming a research hotspot due to its advantages including feasible synthesis procedure, stable physicochemical properties, strong visible light responsibility, high selectivity for H_2O_2 generation, and nontoxicity [13–18]. g-C_3N_4 was firstly employed as photocatalyst for H_2O_2 generation from dioxygen reduction in pure water by Shiraishi [19]. Its mechanism was revealed as follows: Firstly, 1,4-endoxide is formed *via* adsorbing dioxygen into the triazine structure. Then H_2O_2 is generated with a high selectivity after accepting the photo-generated electrons and photons in water. However, the efficiency for H_2O_2 generation always suffers from the fast combination of photo-generated electron and hole pairs. For this issue, various methods were employed to improve the separation efficiency of charge carriers, such as loading noble metal NPs [20], interface modification [21],

* Corresponding authors.
E-mail addresses: zhaoslin@aliyun.com (S. Zhao), Majun0514@sicnu.edu.cn (J. Ma).
[1] These authors contributed equally to this work.

https://doi.org/10.1016/j.cclet.2021.04.028
1001-8417/

heterojunction [22,23]. Among all the attempts, interface modification draws an increasing attention due to its feasible synthesis procedure and satisfactory efficiency. For instance, carbon material, as excellent electron transfer mediation, facilitates the separation of charge carriers. Liu *et al*. reported [24] that ultrathin g-C_3N_4 modified by carbon nanodots exhibited 3.05 times higher activity for H_2 revolution in comparison with unmodified g-C_3N_4 nanosheets. Similarly, Che *et al*. [25] reported that carbon ring modified g-C_3N_4 exhibited 10 times of photocarrier diffusion length and lifetime by relative to pristine g-C_3N_4. Zhao *et al*. [26] reported that g-C_3N_4 combined with carbon nanotubes through amidation reaction exhibited efficient catalytic performance for photocatalytic H_2O_2 production (32.6 μmol/h), even in the presence of formic acid under visible light. Meanwhile, interface modification with trapping regent for photo-formed e^--h^+ pairs, also effectively suppressed the recombination of charge carriers. Yusuke *et al*. [27] reported that g-C_3N_4 doped with biphenyl diimide demonstrated the yield of millimolar levels of H_2O_2 due to the electron-deficient properties of biphenyl diimide. In contrast, boron nitride, as an electron-rich reagent, also improved H_2O_2 yield with solar-to-chemical conversion efficiency of 0.27% [28]. Meanwhile, more negative charges formed on the surface of g-C_3N_4 after modification by potassium hydroxide, which effectively inhibited the recombination of photogenerated electrons and holes, thereby enhancing the yield of H_2O_2 [29].

Although the methods mentioned above all improved the separation efficiency of charge carriers, their migration orientation of carriers are actually different. In terms of the formation process of H_2O_2 production over g-C_3N_4, the number of photogenerated electrons in the triazine structure are directly relative to the migration orientation of carriers, which ultimately determines the H_2O_2 yield. If the electrons are migrated outside of the triazine structure, 1,4-endooxide could not be formed. Thence, it is necessary to clarify the relationship between H_2O_2 yield and migration orientation, which is of great guidance for the development of g-C_3N_4 based photocatalyst with satisfactory performance H_2O_2 generation.

For this emotion, the present work systematically investigated the effect of the migration orientation of charge carriers on the performance of H_2O_2 production. The surface of g-C_3N_4 was modified by electron-rich and electron-deficient material, respectively. The physical-chemical properties, band energy structure, separation efficiency of charge carriers, performance for H_2O_2 production over the surface modified g-C_3N_4 were systematically investigated. It was found that migration orientation of photo-generated electron plays a vital role in the performance for H_2O_2 generation. The research results are of great importance for the design and synthesis of g-C_3N_4 based photocatalyst with high activity for H_2O_2 generation.

Surface modification of UCN by BN and carbon dust were carried out through hydrothermal and calcination method, respectively, as illustrated in Fig. S1 (Supporting information). The performance for H_2O_2 generation over the modified ultrathin g-C_3N_4 was evaluated, as shown in Figs. S1a and b (Supporting information). The activity for H_2O_2 generation over the UCN/BN and UCN/C was quite different. The performance of H_2O_2 production was significantly improved with the increase of BN dosage from 5% to 40%. Only 5.0 μmol/L H_2O_2 could be produced over UCN after 3 h irradiation. In comparison, the H_2O_2 yield over UCN/BN-40% reached 17.0 μmol/L, nearly 4 times higher than that over UCN. However, the activity declined when the BN content increases to be 80%, which may suffer from the inhibited utilization efficiency of light. In contrast, carbon dust modification decreased its activity, *i.e.* 27.1% activity for H_2O_2 generation lost over UCN/C-2%. Meanwhile, UCNBN modification in a small amount also improved H_2O_2 production, while carbon dust loading in a very large amount still decreased H_2O_2 production (Fig. S2 in Supporting information). The improved H_2O_2 production performance over UCN/BN-40% was further verified through investigating production and decomposition rate over the two catalysts, as shown in Fig. S3 (Supporting information). The number of electron transfers (n) is a vital parameter to investigate the selectivity for O_2 reduction. As shown in Fig. 1c, n value over the two catalyst were different. The value over UCN/BN-40% was 1.7, being similar to that over UCN. The two value were close to 2.0, indicating a high selectivity of two-electron reduction for H_2O_2 generation [30]. In contrast, the n value reached as high as 2.7 over UCN/C-2%, demonstrating none-two electron reduction was dominant. The cycle experiments for H_2O_2 generation were shown in Fig. 1d. After successive utilization for 5 times, only 14% of activity decrease was demonstrated, displaying an excellent stability for UCN/BN-40%. The excellent reusability may originate from the strong interaction between BN and UCN in the form of covalent bond. Meanwhile, it was identified the triazine structure was well maintained through X-ray diffraction (XRD), Fourier transform infrared spectroscopy (FT-IR) and X-ray photoelectron spectroscopy (XPS) characterization as shown in Fig. S4 (Supporting information) after the catalyst was reused for 5 times. The decreased activity was ascribed to weight loss of material. Above all, it indicated that the UCN/BN-40% photocatalyst had efficient H_2O_2 production with high stability.

In order to clarify the intrinsic mechanism for the enhanced H_2O_2 generation over UCN/BN, the physicochemical properties and band structure of UCN/BN were systematically analyzed.

The catalyst' morphology and chemistry state were firstly analyzed. As illustrated by scanning electron microscope (SEM) observation (Figs. 2a and b), BN randomly dispersed on the surface of UCN. Since both BN and ultrathin g-C_3N_4 possessed 2D morphology, 2D/2D structure of UCN/BN was feasibly formed. Meanwhile, the amount of BN stacked on the surface of UCN was gradually richer with the increase of BN amount, as illustrated in Fig. 2c, d and Figs. S5a-c (Supporting information). Meanwhile, XPS was adopted to analyze the chemistry state. As shown in survey XPS spectra (Fig. 2e), C, N and O elements were detected over UCN. In comparison, N 1s appeared over UCN/BN-40% as shown in Fig. 2f, indicating the successful loading of BN on the surface of UCN. The loading was further identified by N 1s spectra. The spectra located at 398.6, 399.4 and 401.1 eV were ascribed to sp^2-bonded nitrogen in C=N–C, the N-$(C)_3$ group backbone and the terminal C–N–H, respectively. After BN modification, two peaks appeared at 398.2 and 399.2 eV, being ascribed to N-B bond and C–N–B bond, respectively, indicating that BN was loaded on the surface in the form of C–N–B covalent bond. Noteworthily, a lower binding energy shift occurred for UCN/BN-40% compared with UCN, indicating a strong interaction between the interface between BN and UCN. From the C 1s spectrum and B 1s spectrum, it was confirmed that the structure of UCN was not destroyed after BN loading (Figs. S6a and b in Supporting information). Meanwhile, carbon dust modification did not change the structure of UCN either (Fig. S7 in Supporting information).

Secondly, the structural properties of UCN/BN were analyzed through XRD, FT-IR and Brunauer Emmett Teller (BET) method. As shown in Fig. S8a (Supporting information), two peaks at 27.5° and 13.1° in XRD patters belonged to the characteristic diffraction of (002) and (100) crystal plane of g-C_3N_4. After BN modification, two peaks located at 25.1° and 41.4° appeared, corresponding to (002) and (100) crystal plane of BN. With the increase of BN usage, the intensity of characteristic peak of BN correspondingly decreased due to the reduced mass diffraction of UCN. Meanwhile, three peaks at 810, 1000–1800, 3000–3500 cm^{-1} were observed in FT-IR spectrum (Fig. S8b in Supporting information), which were ascribed to radial respiratory vibration of the triazine ring, telescopic vibration of C=N or C–N bond, and stretching vibration of N–H

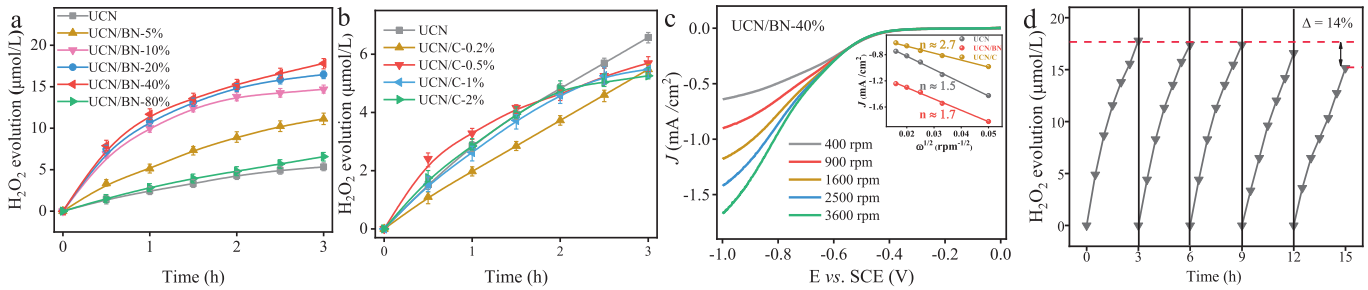

Fig. 1. Photocatalytic performance for H_2O_2 generation over UCN/BN and UCN/C. (a) The effect of BN dosage on the yield of H_2O_2. (b) The effect of C dosage on the yield of H_2O_2. (c) Electron transfer number for UCN/BN-40% and UCN/C-2%. (d) Reusability of UCN/BN-40%.

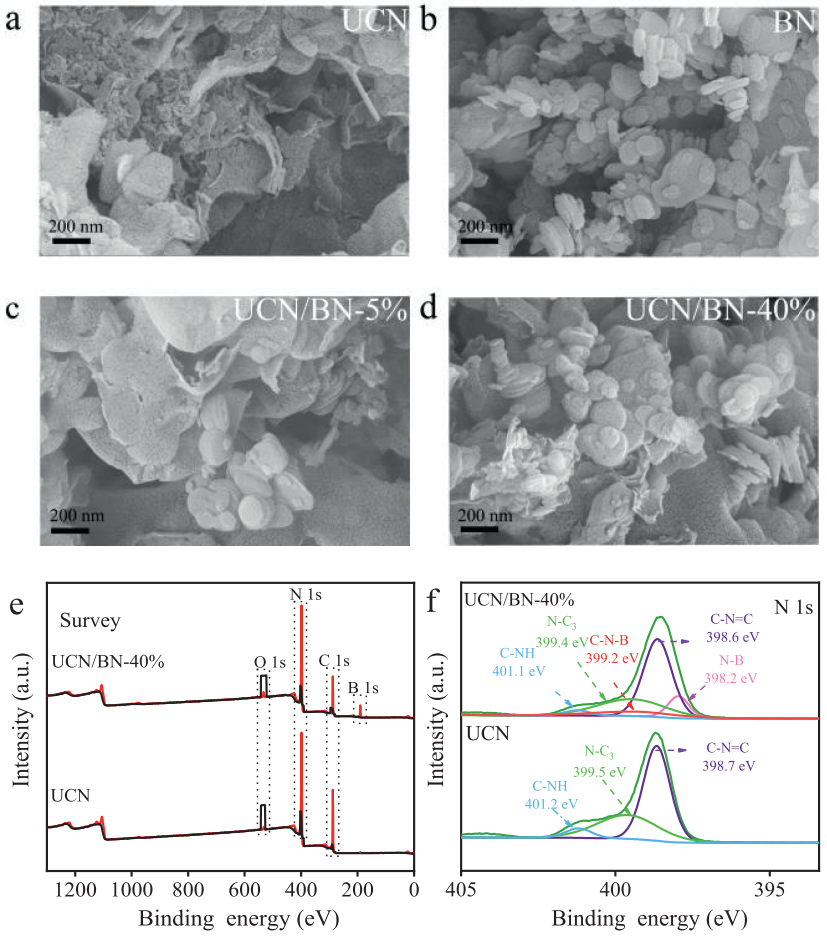

Fig. 2. The morphology and XPS analysis of UCN/BN. SEM image of (a) UCN, (b) BN, (c) UCN/BN-5% and (d) UCN/BN-40%. (e) Survey XPS spectra. (f) N 1s XPS spectra.

bond, respectively. After BN surface modification, the three characteristic peaks were almost unchanged. The specific surface of the catalyst was finally characterized by N_2 adsorption-desorption, as shown in Fig. S8c (Supporting information). All photocatalysts had H_3-type hysteresis loop of N_2 adsorption/desorption isotherms, indicating that the lamellar structure was well maintained. The specific surface area decreased with the BN amount increased, which was not favorable for H_2O_2 generation due to the decreased mass transfer efficiency.

Finally, the band potential of UCN/BN (Fig. S8d in Supporting information) was obtained through combining the UV diffuse reflectance characteristics (Fig. S9 in Supporting information) and Mott-Schottky curve (Fig. S10 in Supporting information). The conduction band (CB) position was almost unchanged, while the valence band (VB) potential of UCN/BN shifted negatively with the amount of BN increased, from 1.962 V *vs.* NHE to 1.563. Theoretically, the lower VB potential of UCN/BN means the poor ability for O_2 reduction due to the reduced oxidation capacity. Therefore, the band structure change was also not ascribed to the enhanced performance.

Besides, the physicochemical and band structure of UCN were also well remained after loading 2% of carbon dust, as illustrated in Figs. S11 and S12 (Supporting information). Thereby, the structural change after surface modification was not the essential reason for the different performance for H_2O_2 production.

It was well known that the photocatalytic activity is highly depended on the separation efficiency of charge carrier [31–34]. Therefore, we reasonably speculated that the opposite performance for H_2O_2 generation originated from the different separation efficiency of charge carriers. Thus, the separation efficiency of charge

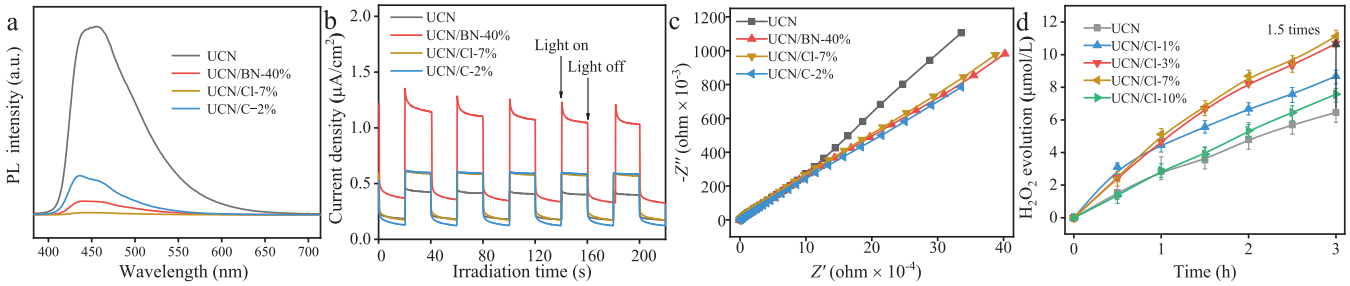

Fig. 3. Separation efficiency of charge carrier and performance for H_2O_2 production over UCN/BN-40%, UCN/C-2% and UCN/Cl. (a) Steady-state photoluminescence spectra. (b) Photocurrent density. (c) Nyquist plots of electrochemical impedance spectroscopy. (d) H_2O_2 evolution over UCN/Cl.

carrier over the modified UCN was investigated through steady-state photoluminescence spectroscopy and photo-current curve measurement. As shown in Fig. 3a**,** the fluorescence intensity of both UCN/BN-40% and UCN/C-2% were significantly lower than that of UCN. Meanwhile, photocurrent intensity over both UCN/BN-40% and UCN/C-2% were remarkably enhanced in comparison with UCN (Fig. 3b). In addition, electrochemical impedance spectroscopy (EIS) Nyquist plots was also analyzed for electrochemical impedance. In Fig. 3c, UCN/BN-40% and UCN/C-2% all demonstrated a smaller EIS Nyquist diagram than UCN under irradiation (Fig. S13 and Table S1 in Supporting information). Hence, it could be concluded that the separation efficiency of charge carrier was all significantly improved for both UCN/BN-40% and UCN/C-2%, indicating that the separation efficiency of charge carrier was also not ascribed to the opposite performance for H_2O_2 generation.

Although both BN and carbon dust could promote the separation of charge carriers, their migration orientation were actually opposite. Photogenerated holes can be attracted by BN because it has electron-rich properties, which makes the holes migrate to the UCN surface [35–38] while leaving the electrons remain inside the triazine structure. It was confirmed that BN attracted holes so that more electrons remained on the UCN. In contrast, it was the holes instead of the electrons, were retained inside the triazine structure, due to the excellent electrical conductivity of the carbon dust. According to the generation mechanism of H_2O_2 over g-C_3N_4, only if more photogenerated electrons were remained inside the triazine structure, more 1,4-endoxides could be formed, thereby producing more hydrogen peroxide. Therefore, it is reasonably speculated that the improved performance for H_2O_2 generation over UCN/BN should be ascribed to the changed migration orientation of charge carriers.

In order to verify the speculation, UCN modified with Cl element was further synthesized since Cl possess the same electron-rich properties as BN [39]. As expected, UCN/Cl demonstrated both enhanced separation efficiency of charge carrier and improved performance for H_2O_2 generation, as shown in Fig. 3. Moreover, the performance for H_2O_2 generation enhanced with the increase of Cl usage. Among all the UCN/Cl catalysts, UCN/Cl-7% demonstrated the optimum activity (Figs. S14a and b in Supporting information), with H_2O_2 evolution almost two-fold than that of UCN after 3 h photocatalytic reaction. Similarly, UCN/Cl-7% demonstrated unchanged physicochemical properties and band structure in comparison with UCN, as shown in Figs. S15-S17 (Supporting information). Therefore, remaining the electrons inside the triazine structure of UCN through attracting hole by electron-rich materials could play a vital role in improving the photocatalytic performance for H_2O_2 generation.

To unambiguously confirm the role of migration orientation of charge carriers, radical trapping experiments were finally conducted, as shown in Fig. 4a. As we all known that EDTA-2Na always acts as an excellent hole-trapping agent [40]. After adding 1 mmol of EDTA-2Na into the reaction system, the performance for H_2O_2 generation over both UCN/BN-40% and UCN/C-2% were significantly improved. Under the same experimental condition, the yield of H_2O_2 increased remarkably from 18.0 mmol/L to 60.0 mmol/L over UCN/BN-40% after 3 h reaction, increased 3.4-fold. Meanwhile, the yield of H_2O_2 also enhanced significantly from 5.0 mmol/L to 17.0 mmol/L over UCN/C-2%, exhibiting a similar growth multiple as UCN/BN-40%. In contrast, adding diphenylamine [41], as an electron-trapping agent, demonstrated an opposite tendency, as shown in Fig. 4b. After adding diphenylamine into reaction system, the yield of H_2O_2 over UCN decreased significantly from 5.0 mmol/L to 2.5 mmol/L. Similarly, the H_2O_2 yield over UCN/BN-40% decreased significantly from 17.0 mmol/L to 5.0 mmol/L, demonstrating a similar activity loss with UCN. The radical trapping experiments results above confirmed the vital role of migration orientation of charge carriers on the performance for H_2O_2 generation.

Based on all the discusses above, the influence mechanism of charge carrier's migration orientation on the performance for H_2O_2 generation was tentatively proposed, as shown in Figs. 4c and d. BN adhered on the surface of UCN can effectively attract photoformed holes due to its electron-rich properties, leading to the enhanced charge separation efficiency, meanwhile remaining more electrons inside of the triazine structure. As a result, the photocatalytic activity for H_2O_2 generation is significantly enhanced since more 1,4-endooxide was formed. In contrast, the photocatalytic activity remarkably decreases over carbon dust modified UCN since photo-generated electrons are attracted outside of the triazine structure. Despite of the improved separation efficiency of charge carriers, electrons finally take part in the formation of $\bullet O_2^-$ radials or H_2O Eqs. 1 and 2 instead of H_2O_2 through none-two electron reduction pathway [42,43].

$$O_2 + e^- \rightarrow \bullet O_2^- \quad (1)$$

$$O_2 + 4e^- + 4H^+ \rightarrow 2H_2O \quad (2)$$

In summary, ultrathin g-C_3N_4 modified by BN and carbon dust, respectively, demonstrated distinctly opposite performance for H_2O_2 generation. Through systematically comparing their separation efficiency of charge carriers, physical-chemical properties and band structure, meanwhile conducting verification and radical trapping experiments, the reason for the opposite performance was reasonably concluded to be ascribed to the migration orientation of charge carriers. The remarkably improved performance for H_2O_2 generation was proved to be the fact that more electrons were remained inside of triazine structure via attracting the photogenerated hole by BN.

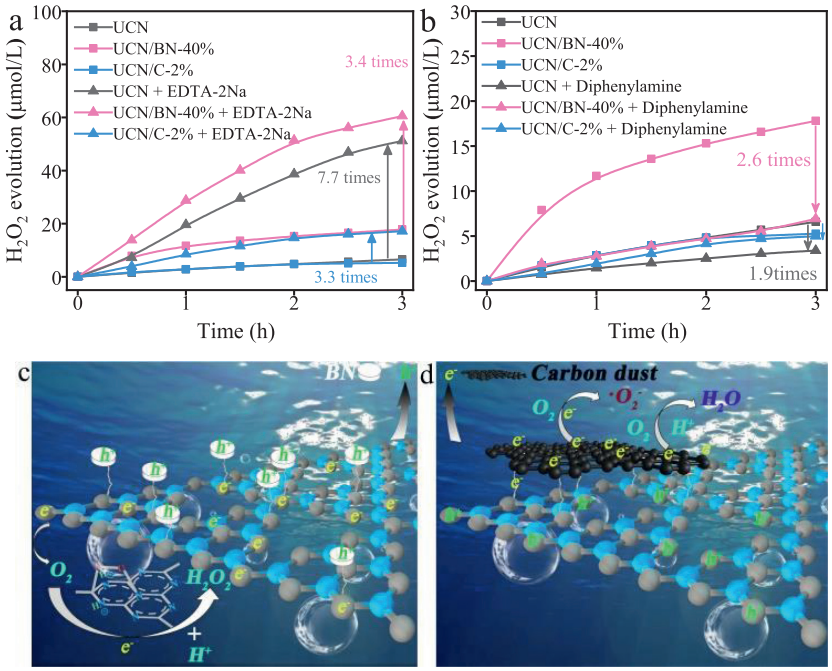

Fig. 4. Schematic diagram for the effect of migration orientation on the H_2O_2 generation over modified UCN. (a) The effect of hole trapping agents on H_2O_2 generation. (b) The effect of electron trapping agents on H_2O_2 generation. (c) Schematic diagram of the possible photocatalytic process of UCN modified by BN under visible light. (d) Schematic diagram of the possible photocatalytic process of UCN modified by Carbon dust under visible light.

Declaration of competing interest

The authors declare that they have no known competing financial interests or personal relationships that could have appeared to influence the work reported in this paper.

Acknowledgments

This work was partly supported by the National Natural Science Foundation of China (No. 21906132), Department of Science and Technology of Sichuan Province (Nos. 2020YFG0158 and 2020YFH0162), and the Engineering Research Center for the Development of Farmland Ecosystem Service Functions, Sichuan Province Institutions of Higher Education.

Supplementary materials

Supplementary material associated with this article can be found, in the online version, at doi:10.1016/j.cclet.2021.04.028.

References

[1] Y. Shiraishi, T. Takii, T. Hagi, et al., Nat. Mater. 18 (2019) 985–993.
[2] L. Chen, L. Wang, Y. Wan, et al., Adv. Mater. 32 (2020) e1904433.
[3] B. Su, R.P. Nia, F. Li, et al., Angew. Chem. 120 (2008) 4753–4756.
[4] J.M. Campos-Martin, G. Blanco-Brieva, J.L. Fierro, Angew. Chem. Int. Ed. 45 (2006) 6962–6984.
[5] J. Ma, K. Wang, C. Wang, et al., Appl. Catal. B: Environ. 276 (2020) 119150.
[6] Y.C. Jin, Y.J. Shi, Z.Y. Chen, et al., Appl. Catal. B: Environ. 267 (2020) 118730.
[7] R. Cao, W. Sun, Z. Zhang, et al., Chin. Chem. Lett. 31 (2020) 3127–3130.
[8] Z. Haider, H.i. Cho, G.h. Moon, H.i. Kim, Catal. Today 335 (2019) 55–64.
[9] L. Zheng, H. Su, J. Zhang, et al., Appl. Catal. B: Environ. 239 (2018) 475–484.
[10] K. Fuku, R. Takioka, K. Iwamura, et al., Appl. Catal. B: Environ. 272 (2020) 119003.
[11] Q.R. Liu, L. Zhou, L. Liu, et al., Composites Part B: Eng. 200 (2020) 108345.
[12] Y.B. Chen, J.F. Li, P.Y. Liao, et al., Chin. Chem. Lett. 31 (2020) 1516–1519.
[13] S. Zhao, X. Zhao, H. Zhang, J. Li, Y.F. Zhu, Nano Energy 35 (2017) 405–414.
[14] Z. Wei, M.L. Liu, Z.J. Zhang, et al., Energy Environ. Sci. 11 (2018) 2581–2589.
[15] L.P. Yang, G.H. Dong, D.L. Jacobs, et al., J. Catal. 352 (2017) 274–281.
[16] Y.L. Yang, M.G. Wu, X.W. Zhu, et al., Chin. Chem. Lett. 30 (2019) 2065–2088.
[17] F. Yang, X.Y. Chu, J.H. Sun, et al., Chin. Chem. Lett. 31 (2020) 2784–2788.
[18] J.Y. Li, Z.Y. Zhang, W. Cui, et al., ACS Catal. 8 (2018) 8376–8385.
[19] Y. Shiraishi, S. Kanazawa, Y. Sugano, et al., ACS Catal. 4 (2014) 774–780.
[20] Y.N. Liu, C.C. Shen, N. Jiang, et al., ACS Catal. 7 (2017) 8228–8234.
[21] J. Wen, J. Xie, H. Zhang, et al., ACS Appl. Mater. Interfaces 9 (2017) 14031–14042.
[22] Y. Yang, Z.T. Zeng, G.M. Zeng, et al., Appl. Catal. B: Environ. 258 (2019) 117956.
[23] S. He, C. Yan, X.Z. Chen, et al., Appl. Catal. B: Environ. 276 (2020) 119138.
[24] Q. Liu, T.X. Chen, Y.R. Guo, Z.G. Zhang, X.M. Fang, Appl. Catal. B: Environ. 193 (2016) 248–258.
[25] W. Che, W. Cheng, T. Yao, et al., J. Am. Chem. Soc. 139 (2017) 3021–3026.
[26] S. Zhao, T. Guo, X. Li, et al., Appl. Catal. B: Environ. 224 (2018) 725–732.
[27] Y. Kofuji, S. Ohkita, Y. Shiraishi, et al., ACS Catal 6 (2016) 7021–7029.
[28] Y. Yang, C. Zhang, D.L. Huang, et al., Appl. Catal. B: Environ. 245 (2019) 87–99.
[29] Y.B. Wang, D. Meng, X. Zhao, Appl. Catal. B: Environ. 273 (2020) 19064.
[30] F.Y. Yu, K. Wang, C. Wang, et al., Chem. Res. Chin. Univ. 36 (2020) 1332–1338.
[31] M.L. Tang, Y.H. Ao, C. Wang, P.F. Wang, Appl. Catal. B: Environ. 270 (2020) 118918.
[32] M.L. Ren, Y.H. Ao, P.F. Wang, C. Wang, Chem. Eng. J. 378 (2019) 122122.
[33] J. Xiong, X.B. Li, J.T. Huang, et al., Appl. Catal. B: Environ. 266 (2020) 118602.
[34] C. Wang, K. Wang, X.X. He, et al., Catal. Lett. 151 (2021) 1225–1230.
[35] D. Tu, H.W. Liao, Q.L. Deng, ChemistrySelect 3 (2018) 7170–7177.
[36] J. Gu, J. Yan, Z. Chen, et al., Dalton. Trans. 46 (2017) 11250–11258.
[37] T. Wang, X.Q. Liu, Q.Y. Men, et al., J. Mol. Liq. 268 (2018) 561–568.
[38] X.W. Lan, Q. Li, Y.Z. Zhang, et al., Appl. Catal. B: Environ. 277 (2020) 119274.
[39] J. Wu, H. Lu, X. Zhang, et al., Chem. Commun. 52 (2016) 5027–5029.
[40] Y.F. Zhang, M.Y. Zhu, S. Zhang, et al., Appl. Catal. B: Environ. 279 (2020) 119390.
[41] C. Karunakaran, R. Dhanalakshmi, P. Gomathisankar, G. Manikandan, J. Hazard. Mater. 176 (2010) 799–806.
[42] C.H. Wang, X.T. Zhang, Y.C. Liu, Appl. Surf. Sci. 358 (2015) 28–45.
[43] J.J. Xu, Y.F. Chen, Z.Y. Dong, et al., Appl. Catal. B: Environ. 252 (2019) 41–46.